HANSER

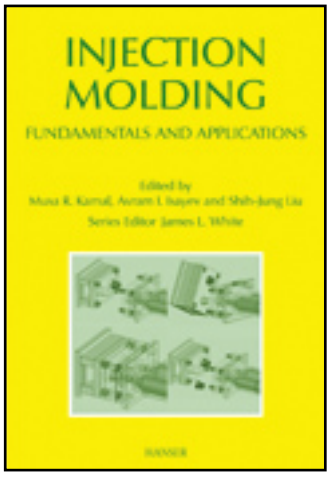

Sample Pages

Injection Molding

Technology and Fundamentals

Herausgegeben von Musa R. Kamal, Avram I. Isayev

ISBN: 978-3-446-41685-7

For further information and order see

http://www.hanser.de/978-3-446-41685-7
or contact your bookseller.

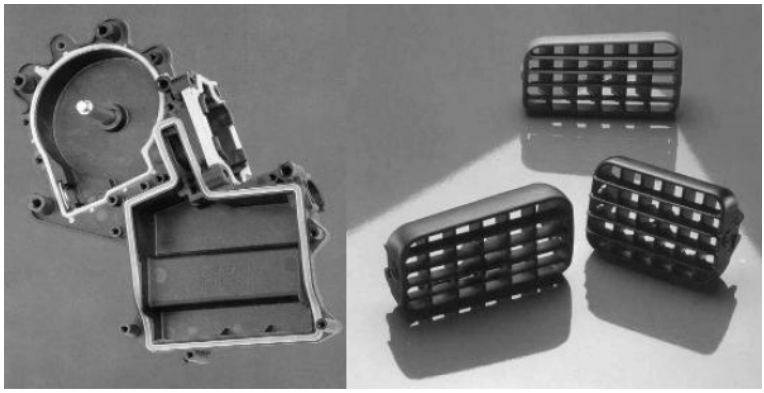

Figure 4.17: Examples of overmolded parts (source: Ferromatik-Cincinnati): (a) overmolded part of two compatible materials; (b) overmolded parts with incompatible materials

4.4 Molds for Injection-Welding

Injection-welding was first developed by Japan Steel Works [11] as a promising solution for molding hollow parts with a complex geometry, with typical applications in the automotive industry. The technology combines a first molding step with an in-mold melt welding operation in one processing cycle, as a competitive alternative to the investment required for costly fusible-core technology. The process involves the molding of two halves of the part (designated as pre-forms); the opening of the mold; a mold movement to place the pre-forms in front of each other; the mold closure; the injection of a welding ring sealing between the two along the grooved border of the pre-forms; and the final opening and ejection of the complete part. The process can also be based on the use of a rotating plate [12], as in the case of the solution proposed for the molding of the bacteriological filter, shown in Fig. 4.18.

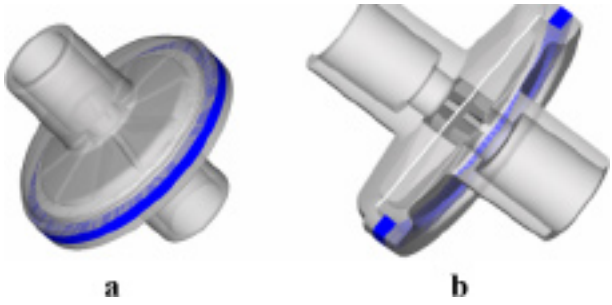

Figure 4.18: Bacteriological filter molded by injection-welding: (a) general view (the welded ring is in blue for better observation); (b) cross-section, showing the position of the inserted paper filter

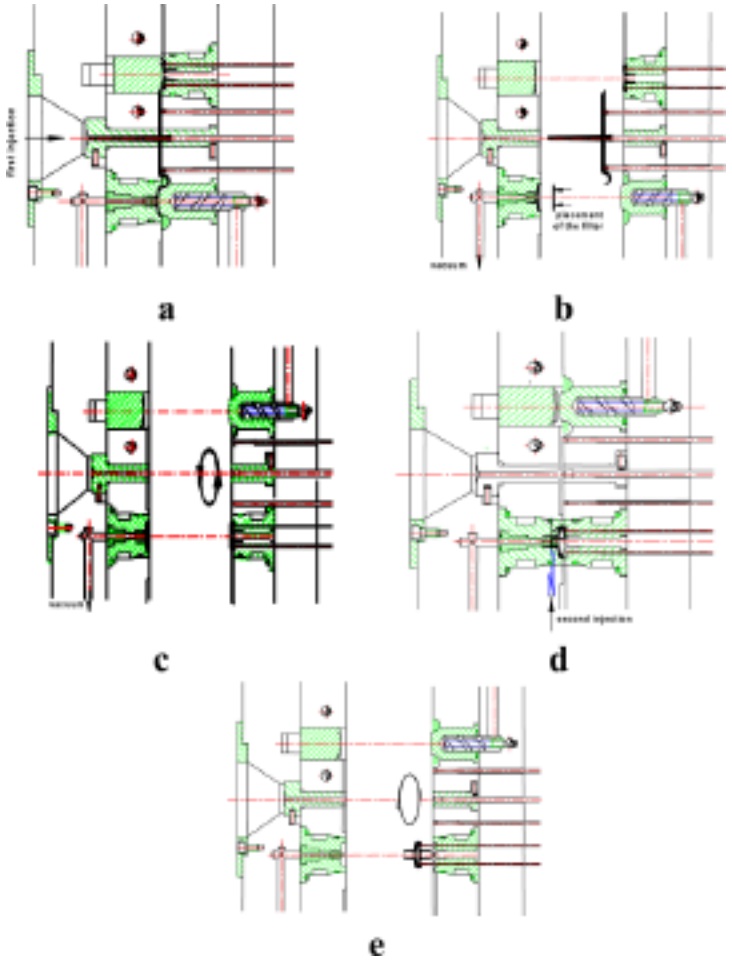

Figure 4.19: Bacteriological filter molded with injection-welding, using a rotating mold: (a) injection of the initial pre-forms of the filter (side gated with a tunnel gate); (b) mold opening and placement of the filtering paper; (c) 180° rotation of the ejection side of the mold, placing the two pre-forms in front of each other; (d) mold closure and injection of the welding ring; and (e) mold opening, ejection of the complete part and subsequent rotation of the mold to its initial position

This solution is detailed in Fig. 4.19, illustrating the sequence of mold movements associated with the different molding steps and placement of the insert. The process can be based on a conventional injection molding machine, with a special cycle programming or in two independent injection units.

The process setup requires the correct adjustment of the material temperature, the injection velocity of the welding ring, and the time gap between the two injections, in order to avoid defects (Fig. 4.20(a) and (b)) and to assure the quality of the welded zone.

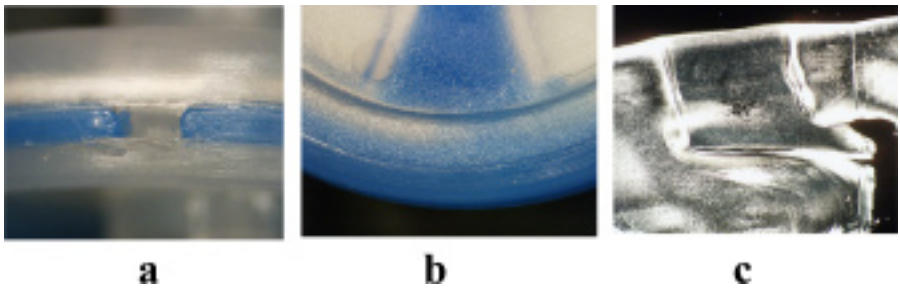

Figure 4.20: Defects in injection-welding and microstructure of the welding zone (moldings in polypropylene with different colors to allow easier visualization): (a) short-shot of the welding ring; (b) internal flash of the welding ring; and (c) microstructure of the welded zone (interfaces between the welding ring and the two pre-forms)

4.5 Molds for Backmolding

Another important family of non-conventional technologies involves the molding of the selected plastic over a layer (or layers) of a functional substrate, previously placed against one molding wall, and is generally designated as backmolding or in-mold lamination. It includes a number of variants, depending on the type of substrate used, namely: molding over textiles or fabrics, molding over a plastic or paper label (in-mold labeling), and molding over a decorative film (in-mold decoration).

4.5.1 Molding over Textiles or Fabrics

This process (Fig. 4.21) involves the placement of a previously cut tissue (e.g., textile, fabric, carpet or leather) geometry on the ejection (moveable) side of the mold and the subsequent injection of the plastic melt over it. Normally, it is performed on conventional injection machines, using a robot to place the textile and remove the final part. However, it is also common to use an injection molding machine with a vertical clamping unit and a rotating table. This equipment allows for easier positioning of the tissue (directly placed on the top of the molding surface) and for the simultaneous development of the complementary operations (textile placement and part removal) within the injection, holding, and cooling stages. This solution requires special tooling with three parts (two moving halves and one injection side) and a side runner system (conventional or hot-runner).

Textile backmolding is widely used by the automotive industry (Fig. 4.22(a)) to produce interior trim components, eliminating the post-operations of cushioning and tissue application onto the molded part. However, it presents several particularities in terms of equipment, tooling and additional operations described below.

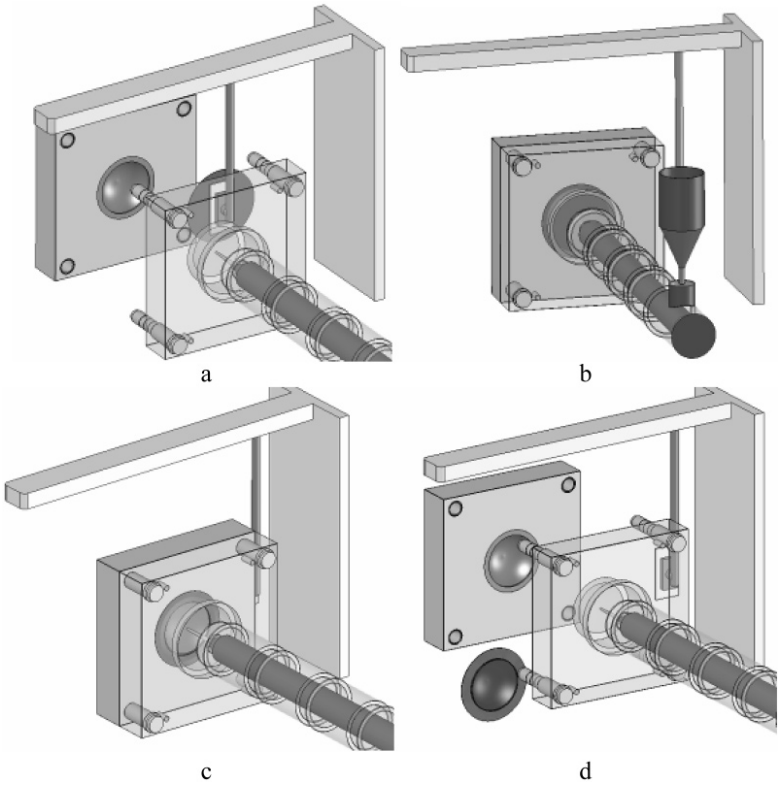

Figure 4.21: Part injected upon the tissue: (a) placement of the textile by the robot; (b) mold closure and fixation of the textile; (c) low pressure injection of the molten polymer; and (d) mold opening and ejection of the complete part (normally, this operation is made by the robot, complementarily to the textile placement)

Figure 4.22: Part injected upon the tissue and mold for textile backmolding (courtesy of Simoldes Plásticos Lda): (a) interior door panel; (b) molding zone (moveable side)

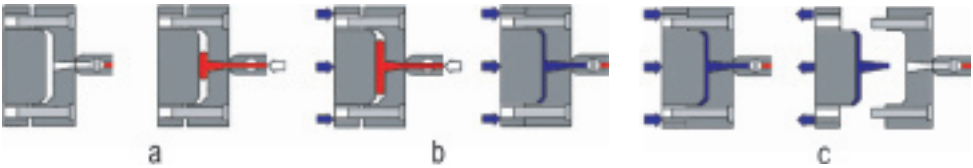

Figure 4.23: Schematic diagram of the injection-compression process: (a) partial mold closure and low pressure injection of the dosed material; (b) initiation of the compression stage and complete mold closure (assuring that material does not return to the plasticating barrel); (c) holding/compression stage and mold opening (with subsequent part removal)

Low Pressure Injection

In order to prevent the loss of the tissue softness caused by the penetration of the plastic melt into the textile structure, low pressure injection molding must be used (although very dependent on the type of tissue selected, cavity injection pressure should not exceed 50 MPa).

Several processing methods can be used to reduce the injection pressure, including,

- injection-compression (initial injection with the mold slightly open, up to 10 mm, followed by the mold closure assuring the complete impression filling by a compression molding mechanism, see Fig. 4.23);
- sequential molding (filling from several valvular hot-runner gates, sequentially opened in a controlled way);
- constant flow front velocity (some injection molding equipment allows accurate adjustment of the velocity of the melt front by variation, up to 50 landings, of the speed of the screw progress. The optimized velocity profile can be achieved directly using commercial process modeling software).

Injection-compression is the more efficient process but limits the options for mold design.

Tissue Selection

In the great majority of cases, the textile substrate is a laminate (or complex) of different layers, including the outside decorative and soft tissue and a protective liner (to prevent the thermal and mechanical damage of the tissue by the molten plastic). It is also common to use a foamed layer for cushioning purposes.

The selected combination of layers (materials and thicknesses) to be used should result from the joint evaluation of the following factors:

- service specifications;
- pressure and thermal loads during the injection and holding stages;
- required deformability of the textile laminate, considering the geometric complexity of the desired part.

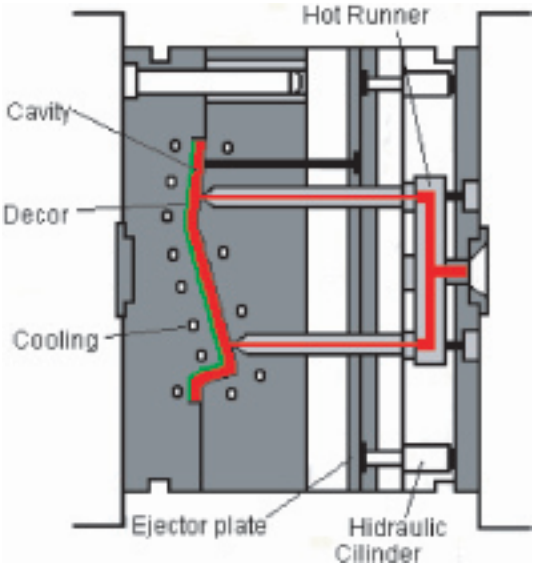

Figure 4.24: Schematic diagram of a mold for tissue backmolding, showing the ejector system on the injection side

Part Geometry

The part design for textile backmolding is a key issue in the process. The part geometry should be adequate to allow the filling with low injection pressure, and the respective contour should be reproduced by the textile (so inner sharp corners and deep depressions should be avoided).

Tissue Fixation

Tissue fixation is normally made by mechanical devices (vacuum is not a suitable solution for permeable textiles). The tissue laminate is firstly placed over some griping points and completely fixed by the mold closure.

Ejection System

Ejector pins should not be operated directly over the tissue surface, as they can damage or mark it, deteriorating its aesthetics. So, the ejection system should operate from the injection side, with the ejectors actuating on the back plastic surface (Fig. 4.24).

Post-Molding Tissue Cutting

Due to fixation reasons and to avoid a visible joint between the covering laminate and the plastic part, the pre-cut tissue has additional peripheral material that should be removed after the molding operation. In fact, the molds should include a zone to accommodate this

10.4.3 Development of Light Induced Reaction Molding (Photomolding) Techniques

Improvements in the above reaction injection molding process were achieved by substitution of slow thermal polymerization by rapid light curing. The following conditions were employed during process development [27]:

- use of mold insert cavities, compatible with the established hot embossing and injection molding equipment
- simple modular construction for short setup times
- comparative constructional elements like in injection molding (ejector pins, runner and gate system, die plate, etc.)
- molding tool evacuation
- optional molding tool temperature control system
- molding under ambient conditions
- low pressure injection for sensitive mold inserts.

The molding equipment was placed in a standard laboratory press, under the lower molding tool, equipped with a glass plate; a powerful UV-source (2.25 kW, intensity up to 1 W/cm^2 at the mold parting surface) was placed underneath. The resin reservoir was directly attached to the upper molding tool, which contained an ejector system and the mold inserts, as well as an integrated runner and gate system. A piston pushes the low viscous resin into the mold cavities, and the injection pressure stays mainly below 20 bars. The individual replication steps are sketched in Fig. 10.9. After closing the molding tool, the mold cavities were evacuated (~1 mbar). Subsequently after injection, a shutter opened and the curing started. Since the polymerization leads to significant shrinkage of the polymer, application of holding pressure during the photopolymerization avoids the generation of sink marks. The final demolding step of the solidified part, using the integrated ejector system, was arranged like a frame around the mold inserts, to finish one replication cycle.

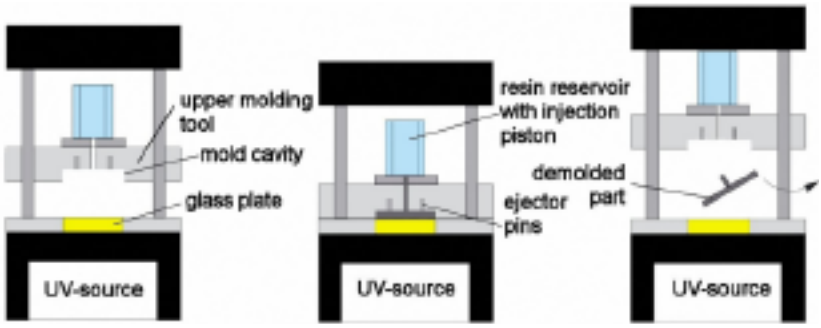

Figure 10.9: Schematic drawing of the photomolding process: closing and evacuation; injection and curing; demolding

The curing time depends strongly on the reactive resin mixture and the additives, especially the concentrations of the photoinitiator and the release agent, as well as on the light intensity. As an example, at constant light intensity, the curing time drops significantly with increasing photoinitiator content until it reaches a local minimum and becomes longer at higher concentrations due to self quenching effects. Additionally, larger photoinitiator amounts cause a increase in brittleness. Therefore, for each system, an optimized photoinitiator content has to be evaluated. The optimized methacrylate based reactive resin mixture allowed the replication of microstructured mold inserts. Figure 10.10 shows in the first row two mold inserts, fabricated by mechanical microengineering and laser-assisted micromachining [28, 29]. As in hot embossing and injection molding, the mold insert surface roughness, especially the side wall roughness, is a good indicator of successful demolding. The test structures in second row of Fig. 10.10 have an aspect ratio of 10 and a width of 35 µm and 40 µm, respectively. The tapered side walls in the mold inserts support demolding.

The realization of high aspect ratio microstructures is important for validation and benchmarking, while microstructures for commercial applications with low aspect ratios between 0.5 and 2 are of certain interest. The use of microfluidic structures in bioanalytics, such as capillary electrophoresis chips or micro titer plates (e.g., at Greiner Bio-One International AG) as well as in micro reaction technology, is commercialized or under investigation [30]. Typical channel structures have a width ranging between 30 and 500 µm and aspect ratios around 1. Figure 10.11 shows some typical structures replicated via photomolding. The left SEM-image shows microfluidic channels for a mixing unit, the right channels are for a tube reactor. The rough sidewalls of the PMMA parts are due to the mold insert fabrication process.

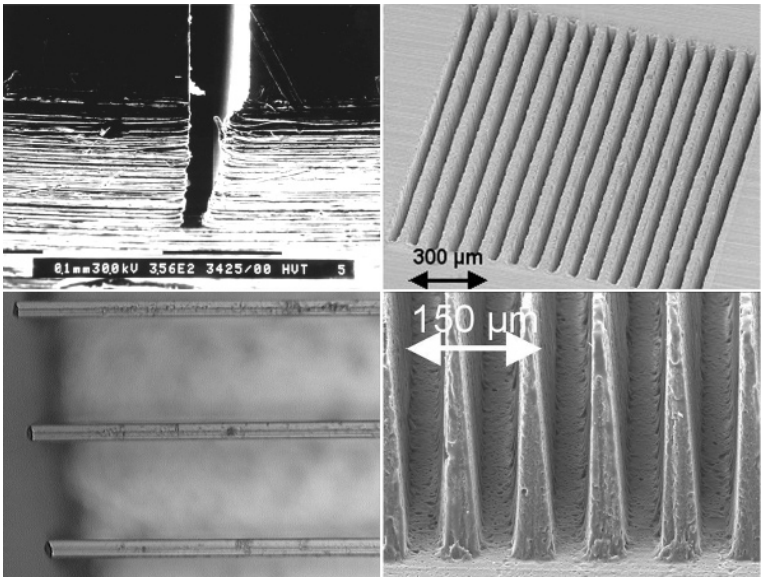

Figure 10.10: Microstructured mold inserts (brass, cemented carbides) and replicated parts (PMMA and polyester) with an aspect ratio of 10

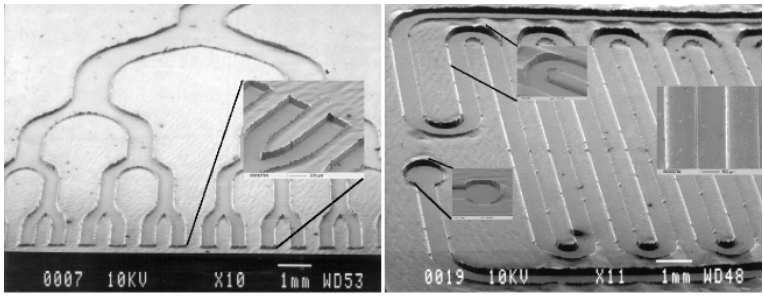

Figure 10.11: SEM-images with of photomolded microfluidic structures [29]

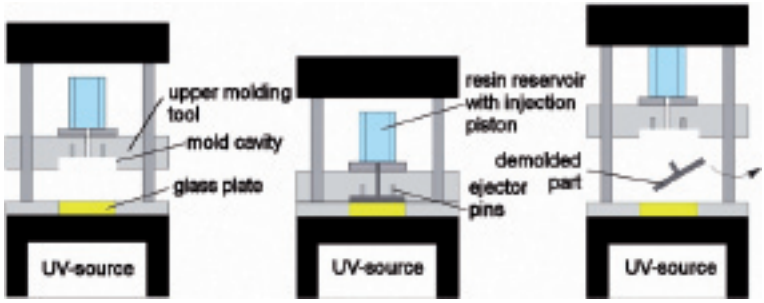

Figure 10.12: Proposed mass production of small parts using light induced reaction molding [33]

The use of laser-assisted micromachining fabricated mold inserts, made of polymers, metals, or ceramics, allows rapid prototyping of polymer microcomponents within two working days [31]. The accessible geometric accuracy of the molded parts is better than 1% [32].

The light induced reaction molding technique should be applicable for mass fabrication. Kobayashi and Shirai [33] suggested a replication technique (Fig. 10.12) for the realization of thin structures with aspect ratios below 1, which shows some similarities to the photomolding process, as described earlier (Fig. 10.9). The metal mold insert is fixed to the lower plate in a small press. The upper plate contains a glass plate with an attached optical fiber, connected to a UV-source. The molding cycle includes three basic steps: application of the curable resin, mold closing and curing, and demolding.

For the replication of microstructures with aspect ratios below 1, an evacuation of the cavities is not necessary. The first molding experiments showed the successful replication of lattice structures with a thickness around 30 μm and structural details around 20 μm [33].

10.4.4 UV-Embossing of Photocurable Systems

Different variants of the UV-embossing technology have been reported in the literature. A thin film or a droplet of UV-curable material (e.g., epoxides, acrylates, urethanes, or curable

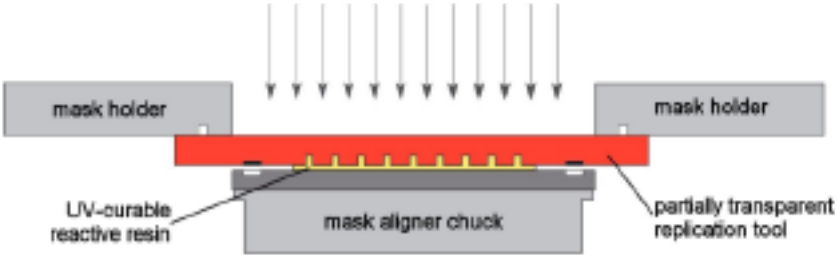

Figure 10.13: Combination of UV-embossing with lithographic techniques [35]

hybride materials such as the sol-gel based ORMOCER's® among others), is placed in a mold, which consists of at least one transparent molding tool [34]. The integration of the molding tool in a mask aligner, normally used in UV-lithography, enables molding on prestructured substrates. A further fusion of UV-lithography with reaction molding is described by Dannberg *et al.* [35] (Fig. 10.13). A partially transparent molding tool (e.g., made of glass or suitable polymers) is used for the microstructuring step. Silicon or glass wafers with alignment marks support the curable material from the back.

The replication process consists of four basic steps:

- mold filling with UV-curable materials (spin coated films, droplets)
- mold closing and embossing
- curing via photopolymerization
- demolding.

The UV-embossing technique is mainly used for the fabrication of a large number of low aspect ratio micro-optical components, such as microlenses for VCSELs, lens arrays, diffractive optical elements (DOE), light concentrators, prisms, OLED lenslets, etc. [34, 35]. Subwavelength elements, such as polarizing structures (metal wire grid) or security features with structural details between 200–400 nm, can be generated using UV-embossing as the replication step [34]. The realization of nanostructures with details around 60 nm, using a patterned quartz mold, is described by Dickey *et al.* [36]. A similar technique is described by Elsner and coworkers [37]. The UV-embossing technique is commercialized under the brand name REEMO by Heptagon, Zurich, Switzerland [38, 39].

The fabrication of thin film high aspect ratio microstructures, using a nickel mold insert and an economic roll-to-roll process, has been described by Chan-Park and Neo [40]. A flexible polyester film carries a solid reactive resin mixture (curable epoxy and urethane acrylate oligomers). The laminate film is pressed against the nickel mold insert (structure height ~50 µm, width ~10 µm, certain side wall inclination angle) using rubber coated rollers for mold filling and then subsequently irradiated for a few seconds. After curing the laminate is peeled off the master (Fig. 10.14, left). The roll-to-roll process enables a low cost mass fabrication of thin polymer film based microstructures (Fig. 10.14, right side). A similar technique for the realization of polymeric microlenses was published by Chang *et al.* [41].

evidence that these threads are not exclusively "manufactured" as a result of local processing conditions. The evidence strongly suggests that they can form upstream (presumably made up of higher molecular weight chains) and transported downstream into their final resting places. Since they possess high orientation and high crystallite sizes, they can survive in their own melt in this very rapid transportation process. The latter phenomenon is optically quite evident in the slow crystallizing polymers discussed below.

17.3.3 Polyoxymethylene (POM) and Other Fast Crystallizing Polymers

The reports on POM [41–44], olefin copolymers [45], and caprolactam [46] indicate that the basic layered morphology described for HDPE and PP above is also observed in these materials:

- a skin layer with lamellae oriented perpendicular to both the mold surface and to the flow direction,
- a so called "transcrystalline layer" with the lamellae oriented perpendicular to the mold surface and twisted around the normal direction, and
- a spherulitic core.

17.3.4 Injection Molded PVDF and its Blends with PMMA

Consistent with the other fast crystallizing polymers, injection molded PVDF samples also exhibit three-layer morphology [47–50]. These include a distinct skin layer formed primarily from chains that have undergone biaxial extensional flow immediately prior to their crystallization upon contact with mold surface. The intermediate layers showing characteristic directional crystal growth were either too thin or were not observed altogether in PVDF. Shear crystallized regions were found to be distinct, and they are followed by the core regions, where the spherulite sizes increase with increasing depth. If the part is thick enough, the spatial variation of spherulites tends to decrease and eventually level off at a certain depth. Wang [51] recently performed extensive investigations on the structure development in injection molded PVDF and its blends with PMMA. He found that addition of PMMA merely lowers the degree of crystallinity [50] and, beyond a concentration of about 35% PMMA, the crystallizability of the blends is greatly diminished even at high shear conditions.

The variation of polymorphism through the thickness direction was investigated using FT-IR technique on microtomed slices [52–61]. This revealed that that the skin layer and the shear zone possess the highest fraction of the β (Form I) crystals, as compared to the core, due to the higher level of stresses experienced by the material in the skin and shear zone during the crystallization process before the cessation of flow.

Micro beam WAXD studies [62] indicate that, at the symmetry midplane of the molded samples, the chains in the skin layer are highly oriented in the direction of flow (Figs. 17.5 and 17.6). The crystal lamellae in this region are mainly extended in the direction per-

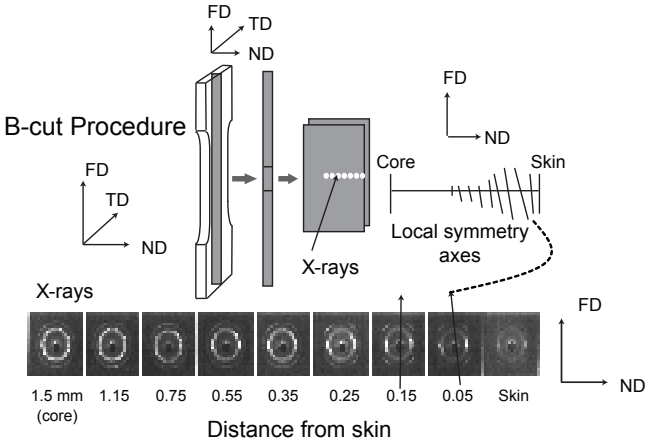

Figure 17.5: Microbeam wide angle X-ray patterns on PVDF injection molded at 40 °C mold temperature with 6.9 cm^3/s injection flow rate [62]

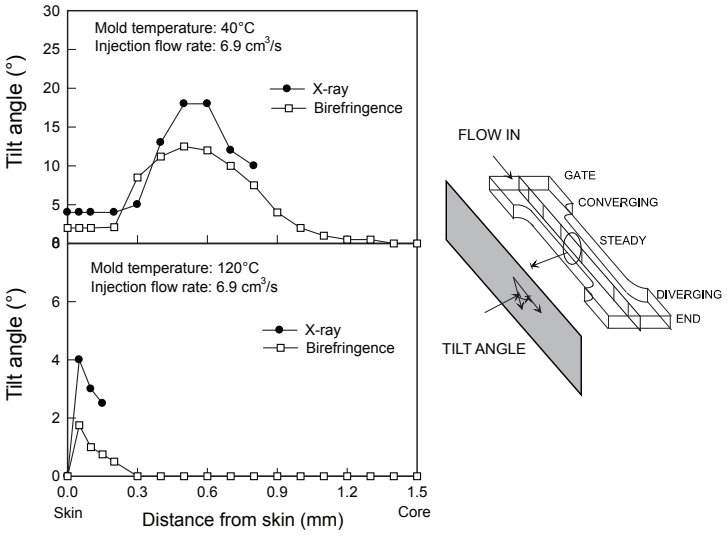

Figure 17.6: Tilt angle as a function of distance from surface measured by microbeam X-ray and birefringence methods [62]

pendicular to the flow direction, as evidenced by the small angle X-ray scattering patterns (Fig. 17.7) [63]. The chains in the shear zone are highly oriented with their local symmetry axis tilted inwards towards the core (Fig. 17.6). This tilting essentially follows the contours of the parabolic velocity profile, suggesting that the orientation profile developed during the injection stage is preserved during the subsequent crystallization stage. The degree of chain axis orientation along the local symmetry axis (close to the flow direction) increases first to

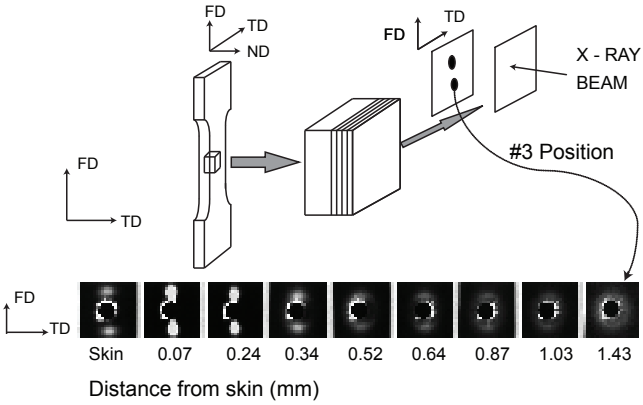

Figure 17.7: SAXS patterns from skin to core. PVDF (mold temp = 40 °C., injection flow rate = 6.9 cm^3/s) [62]

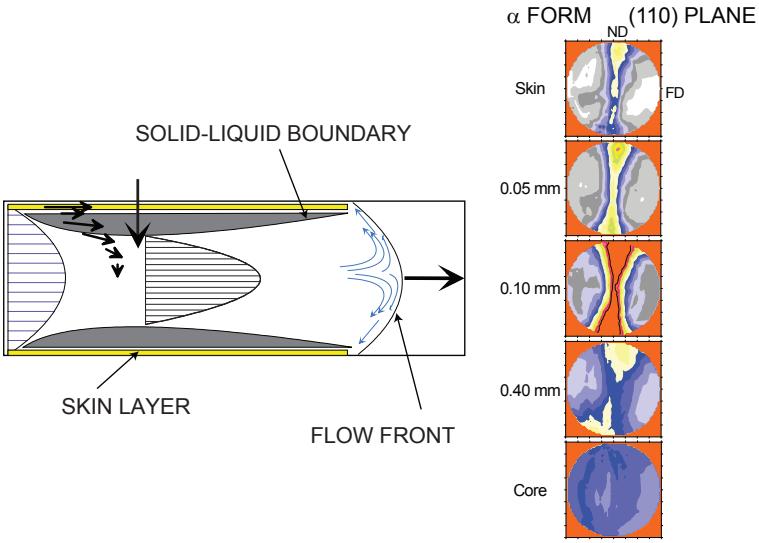

Figure 17.8: Matrixing microbeam pole figures for PVDF injection molded at 40 °C with injection flow rate of 6.3 cm^3/s [62]

reach a maximum level at 0.1 mm from the skin, and then decreases, as the distance from skin increases. In the core, the chains are almost randomly oriented as shown in Figs. 17.8 and 17.9, where the micro beam WAXD pole figures at a series of locations from skin to core are shown as well as the orientation factors that were calculated with respect to their local symmetry axes. In these samples, the spherulitic core is developed mostly after the completion of the injection stage, under no stress or very low level of stress. In the core, the level of molecular orientation is greatly reduced (Fig. 17.6).

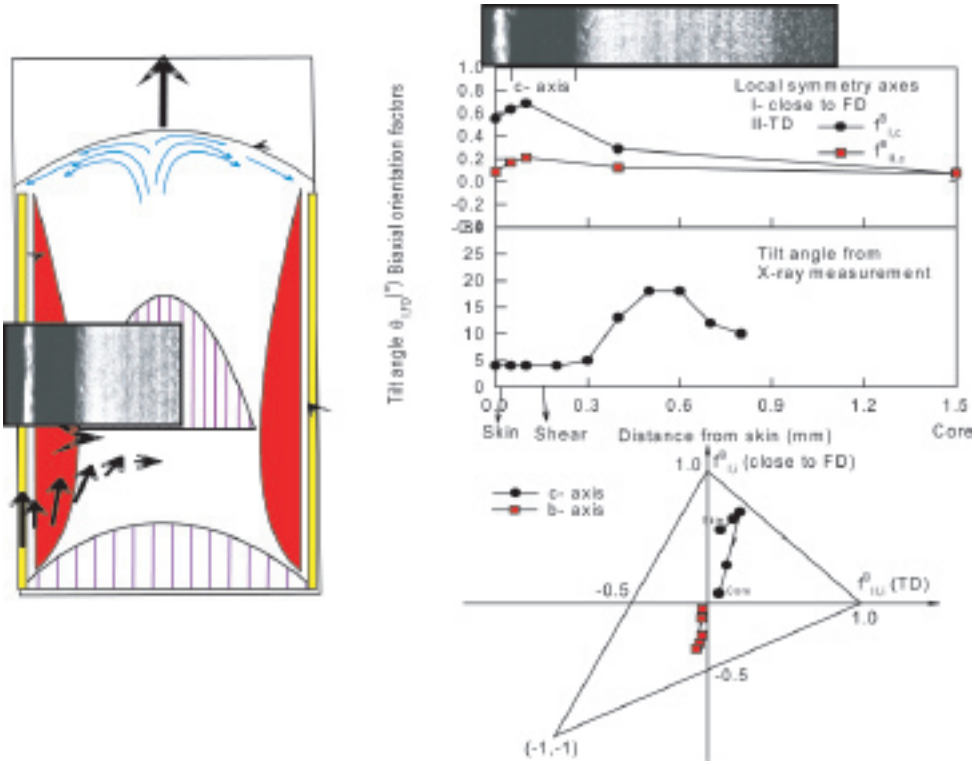

Figure 17.9: Distribution of biaxial orientation factors for PVDF molded at 40 °C mold temperature with 6.9 cm^3/s injection flow rate [62]

The SAXS results revealed that the thickness of the lamellae increases as the distance from the surface increases. Higher mold temperature results in thicker lamellar crystals, due to the relatively high crystallization temperature. The addition of PMMA results in an increase in the long spacing, due to the presence of the PMMA chains in the interlamellar regions (Fig. 17.10).

Micro beam small angle light scattering technique can be used to study the morphological gradient of the injection molded PVDF samples qualitatively at a fairly small step size of about 123 μm as shown in Fig. 17.11. The mold temperature was found to affect the size of the spherulites much more significantly than the injection speed (Fig. 17.12). The higher the mold temperature, the larger are the spherulites at the same distance from the skin, due to the relatively higher crystallization temperature. The addition of PMMA significantly reduced the size of the spherulites, due to the reduced crystallization rates and the increased nucleation density (Fig. 17.13). It should be noted that, for the PVDF/PMMA : 70/30 composition, the spherulites could be observed all the way to skin at high mold temperature (120 °C) and the peak (second data point) was located in the transition layer between the skin and shear layers.

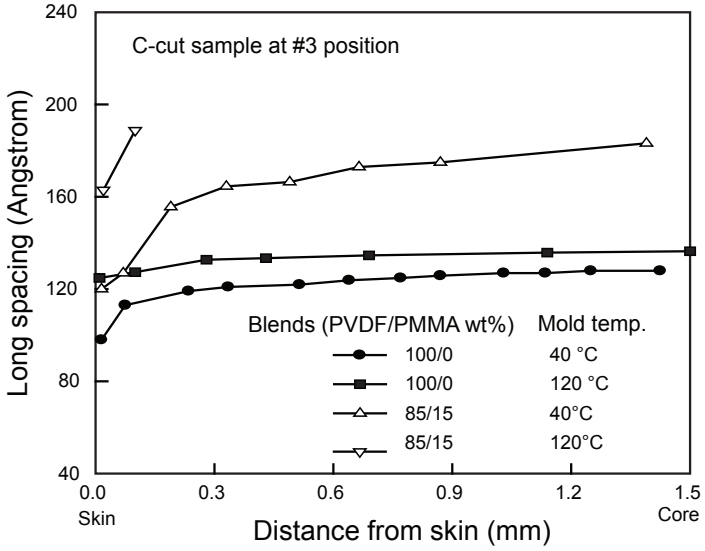

Figure 17.10: Long spacings of PVDF and PVDF/PMMA blends injection molded at 40 and 120 °C measured from skin to core [62]

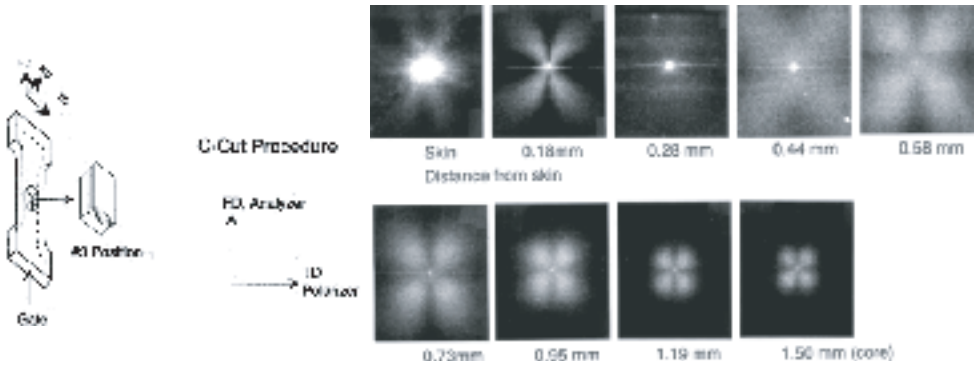

Figure 17.11: SALS Hv patterns of PVDF sample cut with procedure C from skin to core (mold temp: 40 °C, injection speed: 6.9 cm^3/s) [63]

With the addition of PMMA, the size of the spherulites in the core of the samples is reduced, the crystallinities from skin to core are reduced, the spherulites become less perfect, the lamellae become thinner, and the number of the PVDF tie molecules becomes smaller. With the addition of 45 wt.% of PMMA, the injection molded PVDF/PMMA samples become essentially amorphous. Due to the above morphological changes in the molded samples, the stresses at yield and at break of the blends decrease with the increase of the PMMA content, due to the reduced anchoring effect from the PVDF lamellae.

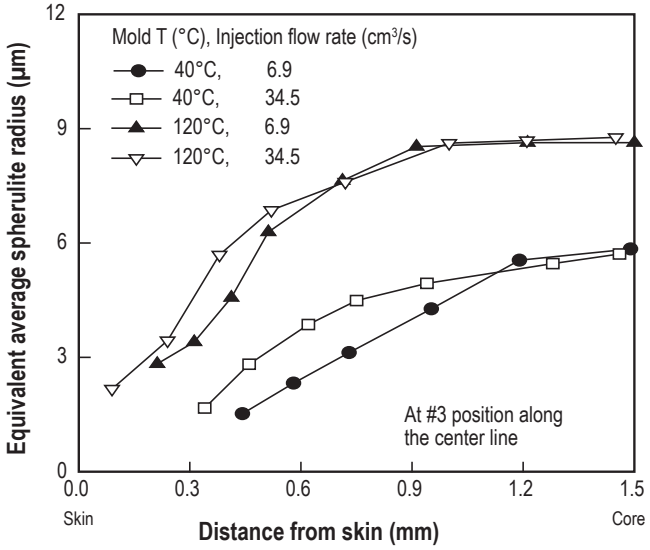

Figure 17.12: Equivalent radius of spherulites vs. distance from skin for PVDF samples molded under different conditions [63]

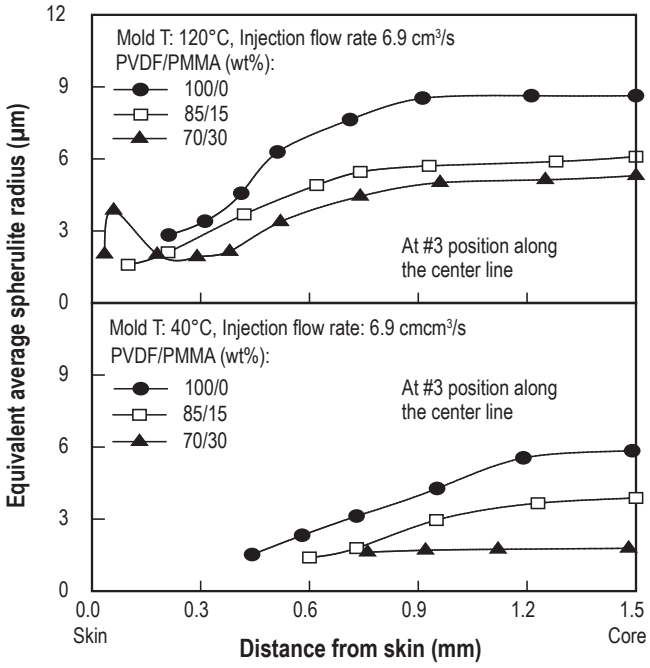

Figure 17.13: Equivalent radius of spherulites vs. distance for PVDF/PMMA samples molded at 40 and 120 °C mold temperatures [63]